

The α Helix Dipole: Screened Out?

Durba Sengupta,¹ Raghu Nath Behera,¹
Jeremy C. Smith,¹ and G. Matthias Ullmann^{1,2,*}

¹IWR—Computational Molecular Biophysics
University of Heidelberg
Im Neuenheimer Feld 368
69120 Heidelberg
Germany

²Structural Biology/Bioinformatics
University of Bayreuth
Universitätsstr. 30, BGI
95447 Bayreuth
Germany

Summary

Aligned α helix peptide dipoles sum to a “macroscopic” dipole parallel to the helix axis that has been implicated in protein folding and function. However, in aqueous solution the dipole is counteracted by an electrostatic reaction field generated by the solvent, and the strength of the helix dipole may reduce drastically from its value in vacuum. Here, using atomic-detail helix models and Poisson-Boltzmann continuum electrostatics calculations, the net effective dipole moment, μ_{eff} , is calculated. Some initially surprising results are found. Whereas in vacuum μ_{eff} increases with helix length, the opposite is found to be the case for transmembrane helices. In soluble proteins, μ_{eff} is found to vary strongly with the orientation and position of the helix relative to the aqueous medium. A set of rules is established to estimate the strength of μ_{eff} from graphical inspection of protein structures.

Introduction

The alignment of the dipoles of peptide bonds in an α helix leads to a “macroscopic” dipole parallel to the helix axis. The strength of this helix dipole is given by the sum of the microscopic dipole moments, μ_i (Creighton, 1993; Hol et al., 1978), arising from the individual peptide bonds, $i = 1, \dots, N$. The magnitude of the vacuum helix dipole is therefore proportional to the number of peptide bonds in the helix (Hol et al., 1978; Wada, 1976) and is approximately equivalent to placing charges of half electron-charge magnitude at the N- and C termini (Sheridan and Allen, 1980; Wada, 1976; Warwicker and Watson, 1982). In proteins, the helix macrodipole has been implicated in function (Hol, 1985) and in stabilizing structural motifs containing helix pairs (Hol et al., 1981; Hol, 1985; Sheridan et al., 1982; Yeates et al., 1987). Furthermore, the helix dipole moment has been suggested to influence pK_a values (Joshi and Meier, 1996), absorption spectra (Lockhart and Kim, 1992), and electron transfer (Galoppini and Fox, 1996) and to stabilize the presence of charged residues at helix termini (Miller et al., 2002).

For a protein in aqueous solution, solvent screening of the peptide group charges is expected to lower the effective dipole of a helix. The screening occurs due to the reaction field of the solvent, which acts against the field generated by the vacuum dipole, leading to an effectively lower dipole moment (Gabdouline and Wade, 1996). However, the magnitude of this screening, and consequently the effective dipole moment is unknown.

For solvent-exposed helical bundles, calculations representing the aqueous medium implicitly have suggested that the helix dipole plays little or no role in stabilizing the observed bundle geometry (Gilson and Honig, 1989). Similar calculations performed on helix pairs in membranes have shown that the electrostatic interaction between helices can be considerable if embedded in the low dielectric region of the membrane, but that the interaction is reduced significantly if the helix termini protrude out into the aqueous phase, even by only a few Ångströms (Ben-Tal and Honig, 1996). Thus, solvent screening is an important factor determining the strength of the interaction between α helices themselves and between α helices and other structural elements in various media.

In the present work, we calculate the effect of the helix environment in screening and modulating the helix dipole. The effective dipole moments, μ_{eff} , of α helices of varying lengths are calculated in vacuum, aqueous solution, lipid bilayers, and protein interiors. μ_{eff} is calculated from the potential generated by the helix, which is represented at atomic detail, in the given environment which is represented implicitly by a continuum model. The helix dipole is relatively strong in vacuum. However, in aqueous solution the helix dipole may be drastically reduced due to an electrostatic reaction field generated by the solvent. Furthermore, whereas in vacuum μ_{eff} increases with helix length, the opposite is found to be the case for transmembrane helices. In soluble proteins, μ_{eff} is found to vary strongly with the orientation and position of the helix relative to the aqueous medium. The results are at first glance surprising, but can be rationalized in terms of the shielding of the helix termini. A set of simple rules is given for estimating μ_{eff} from experimental structures.

Results

Effective Helix Dipole Moment in Homogeneous Media

μ_{eff} of polyalanine helices of various lengths was calculated in vacuum, water, a lipid bilayer, and proteins. The representation of the continuum membrane environment and the globular protein environment used in the paper are shown in Figure 1. In vacuum, the dipole moment of an α helix increases linearly with peptide length (Figure 2A). μ_{eff} calculated from the atomic partial charges, and also that from the fitted charges, is similar to the product of the dipole moment of the peptide group (3.45 D) and the length of the helix, thus demonstrating that the fitting procedure does not introduce unphysical artifacts.

*Correspondence: matthias.ullmann@uni-bayreuth.de

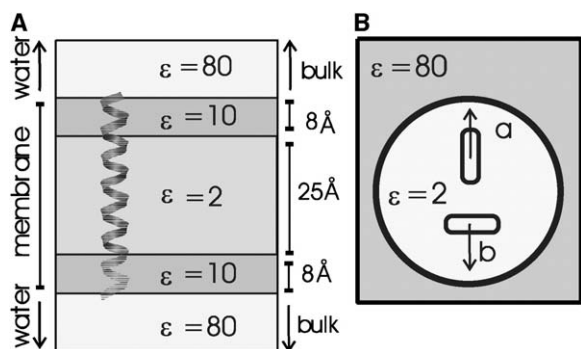


Figure 1. Representation of the Implicit Membrane and Globular Protein Environments

(A) An α helix placed in a five-slab continuum electrostatic model of a biological membrane environment. The membrane is represented as three slabs corresponding to the two head group regions and core region. For more details, see Sengupta et al. (2005).

(B) An α helix in a globular protein depicted as a sphere of low polarity, $\epsilon = 2$. The two orientations in which the helix is placed in the protein correspond to the helix axis (a) along and (b) perpendicular to the radius vector.

In aqueous solution, the solvent reaction field considerably lowers the effective electrostatic potential (Figure 2B). μ_{eff} again increases linearly with peptide length but with a significantly smaller slope than in vacuum. As expected, the screening is even stronger at non-zero ionic strength.

To estimate the magnitude of the reaction field dipole moment arising from the environment, the reaction field potential for helices in water was calculated as the difference of the electrostatic potentials around the helix in water and in vacuum. The helix atom point charges were then fitted to the solvent reaction field potential so as to obtain the effective charges best representing the reaction field. The dipole vectors of the helix in vacuum and the reaction field dipole vectors in aqueous solution are listed in Table 1. The magnitude of the reaction field dipole vector is similar in magnitude to that of the dipole vector of the helix in vacuum but points in the opposite direction. Therefore, the effective dipole vector is the sum of the two nearly equal contributions and is thus very small. Additional calculations (data not shown) demonstrated that μ_{eff} scales with $1/\epsilon$. Thus, in a homogeneous medium all the charges are uniformly screened and the extent of the screening depends only on the polarity of the solvent.

Charge Screening in Membranes

In a heterogeneous environment, such as in a lipid membrane, the situation becomes more complex. μ_{eff} of the helices, now embedded in a membrane with the helix axes perpendicular to the membrane plane, are shown in Figure 3A. μ_{eff} falls off approximately linearly with helix length until the helix spans the membrane (28 residues), at which point the helix dipole moment is reduced to its aqueous solution value and does not change further with further increases in length. This interesting behavior is the opposite of that in uniform media (Figure 2), in which lengthening the helix increases

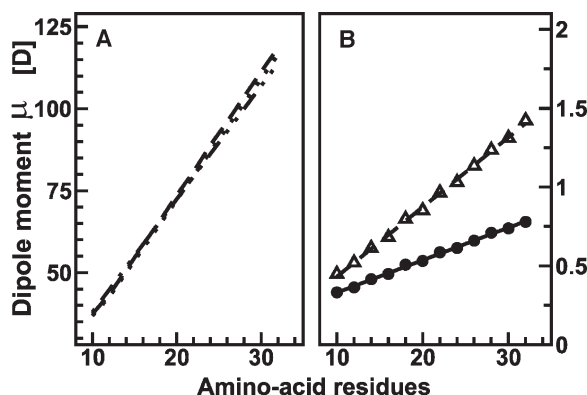


Figure 2. Effective Dipole Moment of Polyalanine Helices in Vacuum and Water as a Function of Peptide Length

(A) Dipole moments calculated using the atomic partial charges (\cdots), calculated by multiplying the 3.45 D peptide bond dipole by the number of peptide bonds ($-\cdots-$), and obtained as the dipole moment of the effective charges obtained from fitting the Poisson potential in vacuum to point charges ($-$). Practically identical results were obtained using effective charges calculated in vacuum with the three-step fitting procedure described in Experimental Procedures, thus demonstrating that the fitting procedure does not introduce unphysical artifacts.

(B) Dipole moments of α helices in water derived from the effective charges calculated by fitting to the Poisson-Boltzmann potential in water at zero ionic strength (Δ) and at 0.15 M ionic strength (\bullet). The solid and dashed lines are linear regression fits to the calculated points.

the dipole moment. The physical origin of the inverse length dependence is revealed by calculating μ_{eff} of a two-charge dipole.

For this calculation, charges of $\pm 0.52e$, generating exactly the helix dipole of the 20-mer in vacuum, were placed at a distance corresponding to the length of the polyalanine helix modeled. A cylinder of diameter 5 Å and dielectric constant $\epsilon = 2$ was placed around the dipole to mimic the associated dielectric boundary. The charged cylinder was placed in the membrane model environment, and the potentials were calculated as above.

As shown in Figure 3A, the length dependence of μ_{eff} for the atomic-detail peptide is reproduced by the two-charge dipole. This observation indicates that the reversal of the slope of μ_{eff} versus peptide length in a membrane is due to the inhomogeneity of the environment. As the peptide length increases, the terminal charges approach the high-dielectric solvent which then screens them. Thus, the reaction field in the surrounding water increases with increasing peptide length, decreasing μ_{eff} .

Most transmembrane helices tilt to varying angles in the membrane. The tilt angle, θ is defined as the angle between the helix axis and the normal to the membrane surface. μ_{eff} versus θ for the 10-mer, 20-mer, and 30-mer polyalanine helices is shown in Figure 3B. $\theta = 0^\circ$ is the orientation in Figure 3A, with the 10-mer and 20-mer buried in the membrane and the 30-mer extending into the aqueous layer. When the helix axis is placed parallel to the membrane plane, i.e., at $\theta = 90^\circ$, the helices are completely embedded in the membrane core.

Table 1. Dipole Moments of Polyalanine Helices in Vacuum and Water

No. of Residues	Dipole Moment [D]		Dipole Moment Vector [D]					
	Water	Vacuum	Vacuum		Reaction Field			
10	0.45	37.4	0.0	-8.0	36.5	-0.0	8.0	-36.0
12	0.5	42.7	4.3	-3.9	42.3	-4.3	3.9	-42.2
14	0.6	50.7	-1.0	2.0	50.7	1.0	-2.0	-50.0
16	0.7	58.5	2.9	-3.9	58.3	-2.9	3.9	-57.6
18	0.8	65.8	2.0	1.0	65.8	-2.0	-1.0	-64.8
20	0.85	73.7	-0.5	-3.9	73.6	0.5	3.9	-74.4
22	0.95	80.8	2.4	-0.5	80.7	-2.4	0.5	-79.6
24	1.0	88.9	-1.4	-2.9	88.8	1.4	2.9	-87.4
26	1.15	96.0	2.9	-2.0	95.9	-2.9	2.0	-95.0
28	1.25	103.7	-1.4	-1.4	103.7	1.4	1.4	-102.2
30	1.3	111.2	2.4	-2.4	112.2	-2.4	2.4	-109.9
32	1.4	118.5	-1.4	-1.0	118.5	1.4	1.0	-116.6

The magnitude and direction of dipole moments of polyaniline helices in vacuum and water is listed. The reaction field vector in water is also given.

Consequently, μ_{eff} is much higher than at $\theta = 0^\circ$ and is approximately equal to μ_{eff} for the corresponding helix in a homogeneous medium of $\epsilon = 2$. As θ increases, so does the shielding of the charges by the reaction field, and hence μ_{eff} decreases. Interestingly, the 30-mer has the largest μ_{eff} when placed parallel to the membrane plane but the smallest μ_{eff} when placed along the membrane normal. Most transmembrane helices have relatively small tilt angles ($\sim 0^\circ$ – 40°), and therefore their corresponding μ_{eff} values will be rather low.

Model Proteins: Principles of Helix Dipole Screening

Extending the analysis to calculate helix dipole strengths in proteins, we first model a globular protein as an uniform sphere of low dielectric constant ($\epsilon = 2$). Two such cases are examined: in one the helix is much shorter than the protein diameter, and in the other the helix spans roughly the entire protein. For both cases,

the helix is buried at varying depths in the protein in the two orientations shown in Figure 1B, i.e., with the helix axis parallel or perpendicular to the sphere radius.

We first consider a decaalanine peptide ($\sim 15 \text{ \AA}$ length) positioned in a protein of radius 25 \AA , corresponding roughly to a molecular weight of 50 kDa. Figure 4 shows μ_{eff} versus the distance d from center of the sphere. In both orientations considered, the reaction field significantly screens the charges of the helix even before it is exposed to the solvent. The screening starts when the helix termini are within $\sim 5 \text{ \AA}$ of the aqueous phase. In the interval $0 < d < 17 \text{ \AA}$, the helix oriented along the radius vector is closer to the solvent than that oriented perpendicularly and is hence shielded more by the reaction field (Case A, Figure 4). However, on increasing the distance from the center, one of the helix termini touches the surface of the sphere and the helix is subjected to a complex dielectric medium with the low dielectric protein at one end and high dielectric water at the other end. The asymmetric reaction field is not able to efficiently stabilize the buried charges and the screening is lower, giving rise to a less steep slope between 17 and 25 \AA (Case C, Figure 4). In the other orientation, with the helix axis perpendicular to the radius vector, the termini of the helix perpendicular to the radius are equidistant from the aqueous phase at all values of d . The reaction field set up at each helix terminus is equal, and μ_{eff} decreases smoothly as the distance from the protein center increases (Case B, Figure 4) until it reaches its value in the aqueous phase (Case D, Figure 4). Figure 4 quantifies how the relative geometries of the helix and the aqueous phase are important in determining the reaction field set up and the extent of the screening of a protein helix.

In a further set of calculations, a 20 residue helix $\sim 30 \text{ \AA}$ length was positioned in a sphere of radius 15 \AA , corresponding roughly to a protein of 10 kDa. μ_{eff} versus the distance from center of the sphere is plotted in Figure 5 for the same two orientations of the peptide as in Figure 4. The same principle holds as for Figure 4, i.e., that the geometry of the aqueous phase around the helix determines the extent to which the μ_{eff} is screened. However, the shape of the plot is different

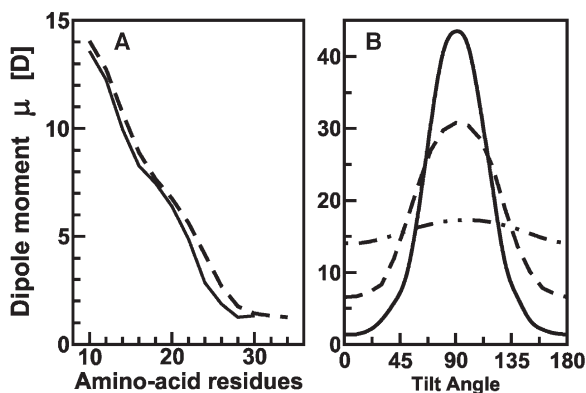


Figure 3. Effective Helix Dipole in Transmembrane Helices
(A) Effective dipole moment of polyaniline helices (—) centered in a five-slab membrane with helix axis parallel to the membrane normal as a function of the peptide length. The dashed line (---) corresponds to the effective dipole moment of a two-charge dipole.
(B) Effective dipole moment of polyaniline peptides centered at the core of a five-slab membrane as a function of the tilt angle, θ . μ_{eff} for polyanilines with 10 residues (···), 20 residues (---), and 30 residues (—) is shown. θ is defined as the angle between the helix axis and the normal to the surface of the membrane.

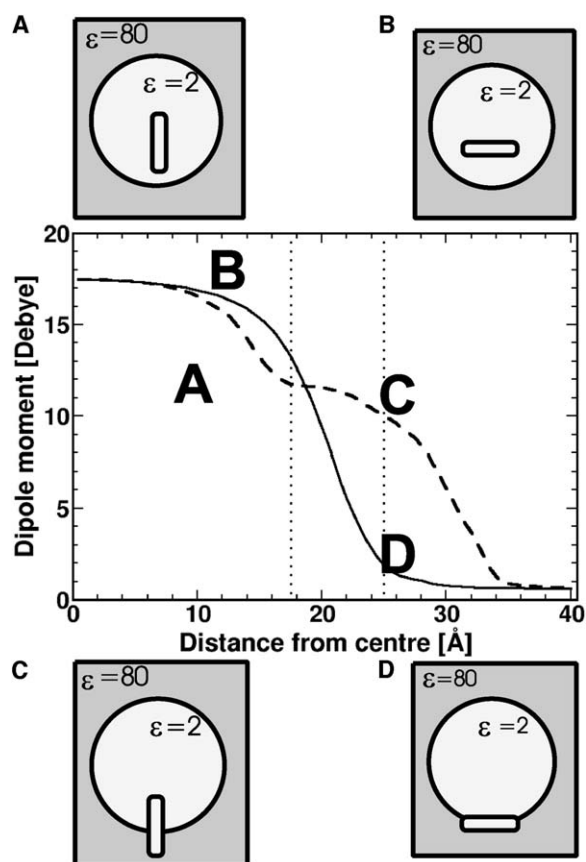


Figure 4. Effective Helix Dipole of a 10-mer Polyalanine Helix in a Large Globular Protein

Effective dipole moment of a decaalanine α helix as a function of the distance from the center of a low-dielectric sphere of radius 25 Å. Two orientations are plotted: helix axis along (---) and perpendicular to (—) the radius. The dotted lines indicate the radius of the sphere (25 Å) and the distance at which the peptide that is along the radius touches the aqueous medium (17.5 Å). The radius also corresponds to the distance at which the center of the helix placed normal to the radius touches the surface of the sphere.

from that of Figure 4. As in Figure 4, the helix perpendicular to the radius vector is screened at both termini uniformly. However, μ_{eff} is roughly constant and significantly smaller since the termini are always very close to the aqueous layer (Cases A and B, Figure 5). In contrast, the helix oriented along the radius vector exhibits complex screening behavior. When the geometric center of the helix coincides with the center of the sphere, both the helix termini are close to the aqueous layer and the helix dipole is screened significantly (Case C, Figure 5). However, when the geometric center of helix is displaced from the center of the sphere, one of the termini is embedded in the low dielectric sphere and hence is poorly shielded. Thus, μ_{eff} increases until the helix terminus coincides with the sphere center (Case D, Figure 5) and then gradually decreases until it is fully exposed to water, when μ_{eff} of the helix is equal to its value in aqueous solution.

Polyalanine helices of varying lengths are now considered in the above globular protein model (radius = 15 Å). The effective dipole moment of the helices is

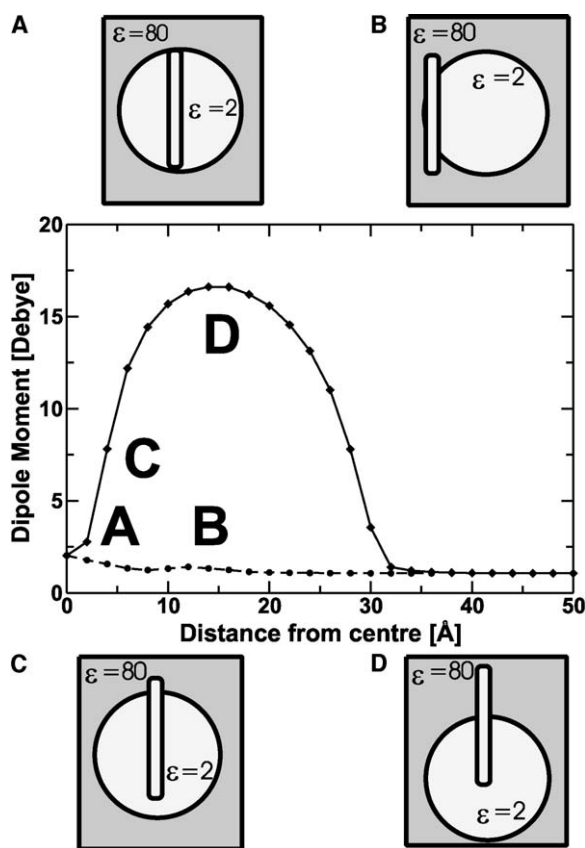


Figure 5. Effective Helix Dipole of a 20-mer Polyalanine Helix in a Small Globular Protein

Effective dipole moment of a 20-mer polyalanine α helix as a function of the distance from the center of a low-dielectric sphere of radius 15 Å. Two orientations are plotted: helix axis parallel (---) and perpendicular (—) to the radius vector.

plotted versus peptide length in Figure 6A. Two positions are considered. In the first position, the helix center of mass is at the protein center of mass. For this position, μ_{eff} decreases as a function of peptide length as the ends of the helices approach the aqueous medium. This behavior is similar to that of helices centered in a membrane (Figure 3A). In the second position, the N-terminal of the helix is placed at the surface of the protein, and the “growing” helix extended into the protein interior. In this orientation, the decamer reaches the center of the protein and the 20-mer spans the entire sphere. In this case, two opposite effects are in play: the increase of dipole moment with increasing number of peptide bonds and the increasing proximity to the aqueous medium of the C-terminal of the helix. For the 12-mer and 14-mer, the C terminus is sufficiently far from the aqueous layer that the dipole moment actually increases as a function of peptide length. However, for the 16-mer and the 18-mer the ends are close enough to the aqueous layer to increase the magnitude of the reaction field, and hence the net μ_{eff} decreases. For the 20-mer both the orientations in Figure 6A coincide and μ_{eff} is the lowest of the cases studied above.

A further interesting case is that of α -helical linkers, linking two domains or two subunits. α -helical linkers

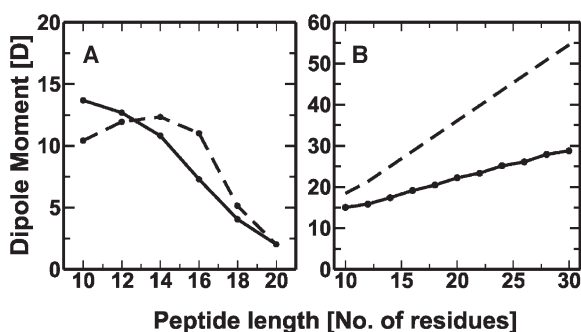


Figure 6. Effective Helix Dipole of Polyalanine Helices in Varying Protein Geometries

(A) Effective dipole moment of polyalanine helices placed along the radius of a low-dielectric sphere of radius 15 Å. The helices are positioned in two ways. In the first, the helix center of mass coincides with the protein center of mass (—). In the second, the N terminus of each helix is placed at the surface of the protein, and the growing helix extends into the protein interior (---).

(B) Effective dipole moment of polyalanine helical linkers. Two low-polarity globular protein models are placed at either end of the helices to model a linker between two domains (—). The corresponding dipole moments in a homogeneous medium of $\epsilon = 2$ are also shown (---).

are important in the calcium binding proteins such as calmodulin. To examine these cases, two globular protein models each of radius 25 Å were placed at either end of polyalanine helices of increasing length. μ_{eff} versus peptide length for helices comprising of 10–30 residues is shown in Figure 6B. μ_{eff} is seen to increase with peptide length, with magnitudes comparable to that in a low-polarity medium, albeit with reduced gradient relative to that of a homogeneous medium of $\epsilon = 2$. The situation of a linker is the reverse of that of the earlier cases, since there is no preferential shielding of the termini, along the length of the helix. Thus, on adding more peptide groups, the terminal charges still experience a medium of low polarity and μ_{eff} increases.

Effective Helix Dipole Moments in Selected Proteins

Finally, we examine atomic-detail models of selected proteins embedded in an $\epsilon = 80$ dielectric continuum (see Experimental Procedures). The proteins and the helices examined are illustrated in Figure 7. The 12 residue α helix in Flap endonuclease corresponds to Case A in Figure 4. The value of μ_{eff} obtained is 17 D, which is about half the in vacuo value and 40 times the value in aqueous solution. This helix dipole is not affected by the aqueous phase, and its electrostatic properties are similar to those in a homogeneous $\epsilon = 2$ continuum. Case C of Figure 4 corresponds to the 9 residue helix of the retinoblastomer protein. Although this helix is strongly solvent exposed $\mu_{\text{eff}} = 10$ D, a value thirty times higher than a fully solvent exposed helix.

Case A of Figure 5 corresponds to proteins such as myoglobin in which the helix spans the entire protein. In this case, solvent screening of the termini considerably lowers the helix dipole of the 26 residue helix to $\mu_{\text{eff}} = 2$ D, which is less than twice the value in water. In contrast, when only one terminus is solvent exposed, corresponding to Case D of Figure 5, the screening is

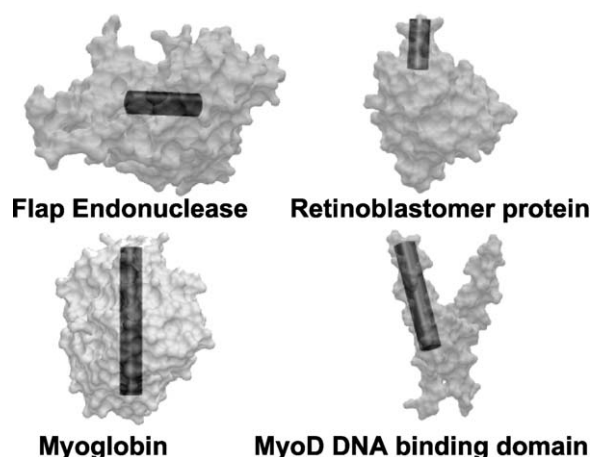


Figure 7. Representation of Helices in Various Proteins Considered in Our Calculations

The cartoon representation of helices considered for calculations in the proteins Flap endonuclease (1A76), retinoblastomer protein (1GUX, chain A), myoglobin (1A6N), and MyoD DNA binding domain (1MDY).

much lower. An example of this geometry is the 27 residue helix in the MyoD DNA binding domain for which $\mu_{\text{eff}} = \sim 23$ D. Extending the analysis to α -helical linkers, the μ_{eff} of the 28 residue linker of calmodulin equals 17 D. In this case only the terminal residues are buried whereas all the nonterminal residues are solvent exposed.

Discussion

The dipole moment of a helix is a macroscopic property that can be used to determine electrostatic interactions at distances that are large compared to the dipole length. Near-field interactions, which would be important in estimates of association free energies, are not accurately represented by the dipole. Thus, the helix dipole is likely to be inadequate for describing effects such as phosphate binding and antiparallel helix motif stabilization. However, a knowledge of the magnitude of the helix macrodipole is of fundamental interest in understanding protein biophysics and macromolecular electrostatics (Creighton, 1993).

The strong vacuum macrodipole is counteracted in aqueous solvent by an electrostatic reaction field due to solvent reorganization. The charge-fitting method presented here has allowed this reaction field and the resulting effective dipole moment μ_{eff} to be estimated for helices in various geometries in proteins and membranes. The calculated effective helix dipole is found to vary considerably in the different geometries and environments considered. For example, in contrast to the common assumption that the helix dipole increases with length, a decrease in helix dipole strength with increasing number of residues is seen in membrane-spanning peptides. Therefore, it is of prime importance to consider μ_{eff} before assigning any structural or functional role to the helix dipole.

The results indicate that the following three rules of

thumb can be used to estimate a helix dipole moment. The rules derived are partly counterintuitive and do not always correspond to common assumptions. First, the dipole strength is determined principally by the positions of the helix termini relative to the aqueous phase. The amount of solvent-exposed surface area does not determine μ_{eff} . In cases where both the termini are buried (at least 7.5 Å from the protein or membrane surface), then the dipole moment is close to that of a helix in a nonpolar medium (e.g., $\epsilon = 2$) and can thus be strong. This rule holds even for helices that, apart from the termini, are solvent exposed, such as helices linking domains as in calmodulin and troponin. μ_{eff} for helices buried in homogeneous apolar media are high. Thus, the corresponding helix-helix interactions are likely to be strong, favoring the antiparallel helix arrangement. An example of this is the antiparallel four-helix bundle motif in cytochrome b562 core (Lange and Hunte, 2002).

The second rule of the thumb is that if both termini are solvent exposed, then μ_{eff} will be small and effectively the same as if the helix were fully solvated in aqueous solution ($\epsilon = 80$). This leads to the observation that μ_{eff} decreases with helix length for transmembrane helices, the opposite length dependence to that in vacuum. This has consequences for de novo protein design, in that elongating an α helix by adding residues with high helix propensity will not necessarily increase the helix dipole. Helices with terminal charges in the aqueous layer and the rest buried in a protein or bilayer core have dipole moments as if they were positioned in only the aqueous phase. Therefore, membrane-spanning helices or helices spanning soluble proteins have small μ_{eff} . Exposure of termini, and therefore low μ_{eff} , may favor parallel arrangement of helix bundles. One example of this is the SNARE complex (Ernst and Brunger, 2003), which is a parallel four-helix bundle with the helices exposed to solvent. Similarly, transmembrane peptides with the termini extending into the aqueous layer can associate in parallel arrangements.

Third, in cases where one helix terminus is solvent exposed and the other buried, asymmetric reaction field shielding can lead to a relatively high μ_{eff} . An interesting example of this is the relatively high dipole moment of the “thumb” of the DNA binding proteins which might contribute to binding to the DNA phosphate groups. Membrane helices with only one pole exposed to the solvent will have relatively large values of μ_{eff} . This may be of functional importance in preventing proton transfer in aquaporin (Tajkhorshid et al., 2002) and for providing ion affinity in the K⁺ channel (Doyle et al., 1998; Roux and MacKinnon, 1999) and the Cl⁻ channel (Faldo-Gomez and Roux, 2004).

Helices with large dipole moments which are not part of helix bundles would be destabilizing in the absence of other stabilizing charged groups. Thus, it is energetically favorable to expose the helix termini to the aqueous layer and shield the helix dipole. For proteins such as myoglobin where the helices have negligibly small dipole moments, it can therefore be postulated that in the folded state there is no contribution of the helix dipole to structural stability.

Helix dipoles are fundamental to protein electrostatics and may contribute to stability and function.

Whether a particular helix has a significant dipole depends on the solvent exposure of the helix termini. The rules of thumb established here allow qualitative estimation of helix dipole strength from graphical inspection of experimental structures.

Experimental Procedures

Standard polyaniline α helices (Creighton, 1993) ($\phi = -57^\circ$, $\psi = -47^\circ$) of 10–34 residues in length were modeled at atomic detail using CHARMM (Brooks et al., 1983). The N- and C termini were blocked with acetyl and N-methyl groups, respectively. All the peptides were energy minimized in a dielectric medium of $\epsilon = 2$ using 1000 steps of “steepest descent” followed by 1000 steps of Newton-Raphson minimization applying harmonic constraints on the backbone atoms (force constant 1 kcal/mol·Å²). The environments of the all-atom helices were represented using continuum electrostatics. Four environments were examined: vacuum, water, protein and a lipid bilayer. μ_{eff} was calculated in a three-step procedure as follows.

Step I: Calculation of the Electrostatic Potential Generated by the Helix

The electrostatic potential around the α -helical peptide was calculated by solving the linearized Poisson-Boltzmann equation numerically using the PBEQ routine (Im et al., 1998) in CHARMM. The vacuum and water dielectric constants were set to 1 and 80, respectively. The calculations were performed at 300 K and 0.15 M ionic strength. The electrostatic potentials were calculated on a grid with cell sizes 1.0, 0.5, and 0.3 Å. The potentials of the coarser grid were used in subsequent focusing onto the finer grids. The distance between the grid boundaries and the peptide surface was at least 12 Å. The charges were taken from the CHARMM force field and the atomic radii were taken as the Born radii (Nina et al., 1997).

A five-slab membrane model (Figure 1A) as introduced in Sen-gupta et al. (2005) was used to calculate the electrostatic potential around helices in a lipid bilayer. In the five-slab model, the dielectric constants for the bulk water, head-group region and membrane core were set to 80, 10, and 2, respectively. The membrane core was 25 Å wide, and both head-group regions were 8 Å in width.

Two models were used to calculate the helix dipole strengths in proteins. In the first, simplified model, a globular protein was represented as a sphere of low polarity with dielectric constant $\epsilon = 2$ (Figure 1B). Two sphere radii were examined: 25 Å, corresponding to a protein of approximately 50 kDa, and 15 Å, corresponding to a protein of ~10 kDa. Outside the spherical region the dielectric constant was set to 80, corresponding to bulk water.

In the second set of protein calculations the whole protein was represented at atomic detail and embedded in an $\epsilon = 80$ continuum phase. The partial charges for only the backbone atoms of the α helix of interest were switched on, whereas the charges on the rest of the protein were set to zero. The dielectric constant of the protein interior was set to 2, and the protein surface was defined as the water-accessible surface. The potential arising from the helix backbone atoms was calculated on grid points up to a distance of 4.5 Å from the helix and outside the van der Waals radii of the helix atoms. The proteins and their corresponding helices used for these all-atom calculations were as follows: Flap endonuclease (PDB code: 1A76 [Berman et al., 2000]; residues 58–70), retinoblastomer protein (PDB code: 1GUX; residues 569–577), myoglobin (PDB code: 1A6N; residues 124–149), MyoD DNA binding domain (PDB code: 1MDY; residues 194–220), calmodulin (PDB code: 3CLN; residues 69–96).

Step II: Fitting Atomic Point Charges to the Electrostatic Potential

Effective atomic point charges, q_i^{eff} , of the helix atoms were obtained by adjusting the charges to reproduce the electrostatic potential generated in Step I. The fitting was performed using a least-squares procedure similar to CHELPG (Breneman and Wiberg, 1990) in combination with singular value decomposition. The electrostatic potentials were mapped to a grid with 0.3 Å grid spacing.

All points up to a distance of 4.5 Å from the molecule but outside the atomic van der Waals radii were included. The total charge of the helix was constrained to be zero.

Step III: Dipole Moment Calculation

In the third and final step, the magnitude and the direction of the effective dipole was calculated as $\mu_{\text{eff}} = q_i^{\text{eff}} r_i$, where r_i is the position of atom i of the helix.

Received: November 5, 2004

Revised: February 16, 2005

Accepted: March 16, 2005

Published: June 7, 2005

References

- Ben-Tal, N., and Honig, B. (1996). Helix-helix interaction in lipid bilayers. *Biophys. J.* **71**, 3046–3050.
- Berman, H.M., Westbrook, J., and Feng, Z. (2000). The Protein Data Bank. *Nucleic Acids Res.* **28**, 235–242.
- Breneman, C., and Wiberg, K.J. (1990). Determining atom-centered monopoles from molecular electrostatic potentials: need for high sampling density in conformational analysis. *J. Comp. Chem.* **11**, 361–373.
- Brooks, B.R., Bruccoleri, R.E., Olafson, B.D., States, D.J., Swaminathan, S., and Karplus, M. (1983). CHARMM: a program for macromolecular energy, minimization, and dynamics calculation. *J. Comp. Chem.* **4**, 187–217.
- Creighton, T.E. (1993). *Proteins: Structures and Molecular Properties* (New York: WH Freeman and Co.).
- Doyle, D.A., Cabral, J.M., Pfuetzner, R.A., Kuo, A., Gulbis, J.M., Cohen, S.L., Chait, B.T., and MacKinnon, R. (1998). The structure of the potassium channel: molecular basis of K⁺ conduction and selectivity. *Science* **280**, 69–77.
- Ernst, J.A., and Brunger, A.T. (2003). High resolution structure, stability and synaptotagmin binding of a truncated neuronal snare complex. *J. Biol. Chem.* **278**, 8630–8636.
- Faraldo-Gomez, J., and Roux, B. (2004). Electrostatics of ion stabilization in a clc chloride channel homologue from *Escherichia coli*. *J. Mol. Biol.* **339**, 981–1000.
- Gabdouline, R.R., and Wade, R.C. (1996). Effective charges for macromolecules in solvent. *J. Phys. Chem.* **100**, 3868–3878.
- Galoppini, E., and Fox, M.A. (1996). Effect of the electrical field generated by the helix dipole on photoinduced intramolecular electron transfer in dichromorphic α -helical peptides. *J. Am. Chem. Soc.* **118**, 2299–2300.
- Gilson, M.K., and Honig, B. (1989). Destabilization of an α -helix bundle protein by helix dipoles. *Proc. Natl. Acad. Sci. USA* **86**, 1524–1528.
- Hol, W.G.J. (1985). Effects of the α -helix dipole upon the functioning and structure of proteins and peptides. *Adv. Biophys.* **19**, 133–165.
- Hol, W.G.J., van Duijjen, P.T., and Berendsen, H.J.C. (1978). The α -helix dipole and the properties of proteins. *Nature* **273**, 443–446.
- Hol, W.G.J., Halie, L.M., and Sander, C. (1981). Dipoles of the α -helix and β -sheet: their role in protein folding. *Nature* **294**, 532–536.
- Im, W., Beglov, D., and Roux, B. (1998). Continuum solvation model: computation of electrostatic forces from numerical solutions to the poisson boltzmann equation. *Comp. Phys. Commun.* **109**, 1–17.
- Joshi, H.V., and Meier, M. (1996). The effect of a peptide helix macrodipole on the pKa of an asp side chain carboxylate. *J. Am. Chem. Soc.* **118**, 12038–12044.
- Lange, C., and Hunte, C. (2002). Crystal structure of the yeast cytochrome bc1 complex with its bound substrate cytochrome c. *Proc. Natl. Acad. Sci. USA* **99**, 2800–2805.
- Lockhart, D.J., and Kim, P.S. (1992). Internal stark effect measurement of the electric field at the amino terminus of an alpha helix. *Science* **257**, 947–951.
- Miller, J.S., Kennedy, R.J., and Kemp, D.S. (2002). Solubilized, spaced polyalanines: a context-free system for determining amino acid α -helix propensities. *J. Am. Chem. Soc.* **124**, 945–962.
- Nina, M., Beglov, D., and Roux, B. (1997). Atomic born radii for continuum electrostatic calculations based on molecular dynamics. *J. Phys. Chem.* **101**, 5239–5248.
- Roux, B., and MacKinnon, R. (1999). The cavity and pore helices in kcsa K channel: electrostatic stabilization of monovalent cations. *Science* **285**, 100–102.
- Sengupta, D., Meinhold, L., Langosch, D., Ullmann, G.M., and Smith, J.C. (2005). Understanding the energetics of helical-peptide orientation in membranes. *Proteins* **58**, 913–922.
- Sheridan, R.P., and Allen, L.C. (1980). The electrostatic potential of the alpha helix. *Biophys. Chem.* **11**, 133–136.
- Sheridan, R.P., Levy, R.M., and Salemme, F.R. (1982). α -helix dipole model and electrostatic stabilization of 4- α -helical proteins. *Proc. Natl. Acad. Sci. USA* **79**, 4545–4549.
- Tajkhorshid, E., Nollert, P., Jensen, M., Miercke, L.J.W., O'Connell, J., Stroud, R.M., and Schulten, K. (2002). Control of the selectivity of the aquaporin water channel family by global orientational tuning. *Science* **296**, 525–530.
- Wada, A. (1976). The alpha helix as an electric macro dipole. *Adv. Biophys.* **9**, 1–63.
- Warwicker, J., and Watson, H.C. (1982). Calculation of the electric potential in the active site cleft due to α -helix dipoles. *J. Mol. Biol.* **157**, 671–679.
- Yeates, T.O., Komiya, H., Rees, D.C., Allen, J.P., and Feher, G. (1987). Structure of the reactions center from *Rhodobacter sphaeroides* r-26: membrane-protein interactions. *Proc. Natl. Acad. Sci. USA* **84**, 6438–6442.